

Scalable and Chemoselective Synthesis of γ -Keto Esters and Acids via Pd-Catalyzed Carbonylation of Cyclic β -Chloro Enones

Justin M. Kaplan,[†] Damian P. Hruszkewycz,[†] Iulia I. Strambeanu,[†] Christopher J. Nunn,[‡] Kelsey F. VanGelder,[†] Anna L. Dunn,[†] Derek I. Wozniak,[§] Graham E. Dobereiner,[§] and David C. Leitch^{*,†}

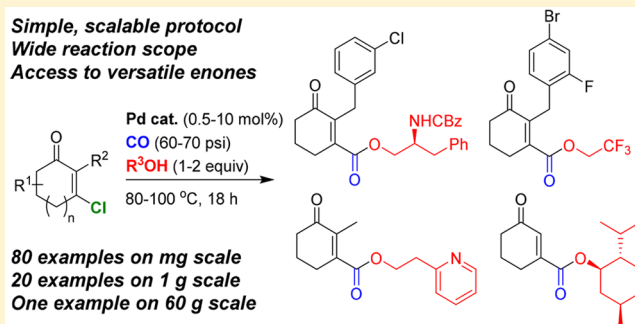
[†]API Chemistry, GlaxoSmithKline, King of Prussia, Pennsylvania, United States

[‡]Product and Process Engineering, GlaxoSmithKline, King of Prussia, Pennsylvania, United States

[§]Department of Chemistry, Temple University, Philadelphia, Pennsylvania, United States

Supporting Information

ABSTRACT: The Pd-catalyzed carbonylation of cyclic β -chloro enones using simple phosphine ligands is described. Screening identified $P(\text{Me})(t\text{-Bu})_2$ as the most general ligand for an array of chloro enone electrophiles. The reaction scope has been evaluated on a milligram scale across 80 examples, with excellent reactivity observed in nearly every case. Carbonylation can be achieved even in the presence of potentially sensitive or inhibitory functional groups, including basic nitrogens as well as aryl chlorides or bromides. Twenty examples have been run on a gram scale, demonstrating scalability and practical utility. Using $P(\text{Me})(t\text{-Bu})_2$, the reaction rate depends on both nucleophile and electrophile identity, with completion times varying between 3 and >18 h under a standard set of conditions. Switching to $P(t\text{-Bu})_3$ for the carbonylation of 3-chlorocyclohex-2-enone with methanol results in a dramatic rate increase, enabling effective catalysis with kinetics consistent with rate-limiting mass transfer. Stoichiometric oxidative addition of 3-chlorocyclohex-2-enone and 3-oxocyclohex-1-enecarbonyl chloride to both $\text{Pd}[P(t\text{-Bu})_3]_2$ and $\text{Pd}(\text{PCy}_3)_2$ has enabled characterization and isolation of several potential catalytic intermediates, including Pd–vinyl and Pd–acyl species supported by $P(t\text{-Bu})_3$ and PCy_3 ligands. Monitoring the oxidative addition of 3-chlorocyclohex-2-enone to $\text{Pd}(\text{PCy}_3)_2$ by NMR spectroscopy indicates that coordination of the alkene precedes oxidative addition. As a result of these studies, methyl 3-oxocyclohex-1-enecarboxylate has been synthesized via Pd-catalyzed carbonylation of 3-chlorocyclohex-2-enone in 90% yield on a 60 g scale with only 0.5 mol % catalyst loading.



INTRODUCTION

Metal-catalyzed carbonylation is a powerful and extensively applied method for the introduction of CO as a C_1 unit into organic compounds.¹ The current abundance of CO available from methane, the promise of carbon-neutral reductions of CO_2 to CO,² and the excellent atom economy of many carbonylation reactions make CO the ideal ambiphilic C_1 source. It is therefore no surprise that carbonylative processes are among the highest volume applications of homogeneous catalysis in industry.^{3,4} In the fine chemical, agrochemical, and pharmaceutical sectors, Pd-catalyzed carbonylation is an efficient and direct method to construct aldehyde, ketone, and carboxylic acid derivatives in a single multicomponent reaction.⁵

Many Pd-catalyzed cross-couplings can be modified to perform as carbonylations; however, CO forms very strong bonds with Pd(0), occupying a coordination site and stabilizing the low oxidation state through synergistic bonding. This raises energy barriers for the oxidative addition of C–X bonds, often making this step turnover limiting in carbonylation catalysis.^{5–7} As a result, the vast majority of reported Pd-catalyzed carbonylations

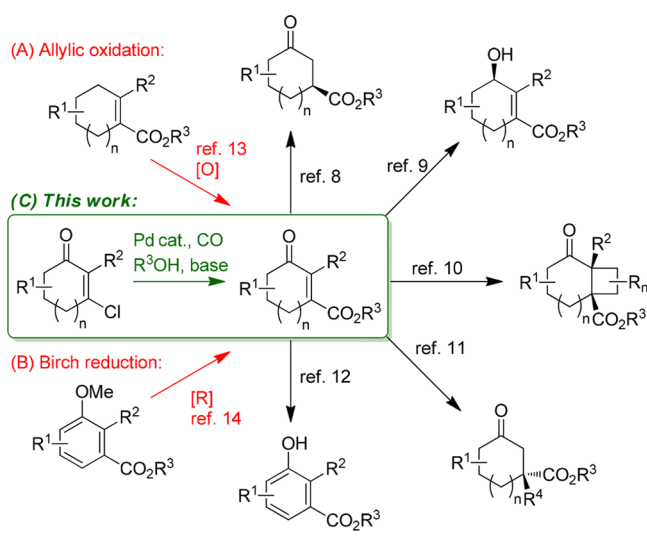
use substrates with weaker aryl or vinyl C–I bonds; effective use of unactivated aryl or vinyl chlorides is considerably rarer.^{5,7} Unfortunately, the stepwise installation and subsequent elimination of iodide is not mass efficient, making Pd-catalyzed carbonylation unattractive from an economic and environmental perspective. Even in the few reported carbonylations of unactivated aryl or vinyl chlorides,⁷ the generally high reaction temperatures and relatively narrow substrate scope limit practical applications in the preparation of functionally complex molecules.

During chemical development for a clinical candidate API, we required rapid access to large quantities of several cyclic γ -keto ester derivatives. A survey of existing methods to prepare these compounds revealed that allylic oxidation using CrO_3 is nearly universally preferred,^{8–13} despite the environmental and

Special Issue: The Roles of Organometallic Chemistry in Pharmaceutical Research and Development

Received: July 5, 2018

Scheme 1. Approach to γ -Keto Esters via Carbonylation and Examples of the Synthetic Versatility of These Products



safety issues with use of Cr(VI) reagents (Scheme 1A). This method would also be incompatible with substrates containing other oxidizable sites, such as where R^2 = alkyl. An alternative approach involves Birch reduction of *m*-anisic acid derivatives,¹⁴ which also carries significant safety, scalability, and chemoselectivity concerns (Scheme 1B). We therefore sought both a versatile, redox-neutral synthetic method in the near term and a viable long-term solution to access these compounds on scale.

Herein we describe the development of the Pd-catalyzed carbonylation of readily accessible cyclic β -chloro enones to access highly versatile^{8–12} α,β -unsaturated γ -keto esters and acids in high yield with a broad substrate scope (Scheme 1C). We hypothesized that the activated nature of the chloro enone moiety (a vinylogous acid chloride) would enable effective oxidative addition even in the presence of CO. Accordingly, these carbonylations give good to excellent yields without the need for the alcohol substrate to be used as the solvent.⁵ Carbonylation of α -substituted β -chloro enones (easily accessed via alkylation or arylation of the precursor diones) generates highly functionalized tetrasubstituted alkenes. Chemoselective carbonylation at the vinyl chloride position is possible in the presence of a variety of functional groups, including aryl chlorides or bromides. Finally, these reactions proceed at practical rates with catalyst loadings as low as 0.5 mol %.

RESULTS AND DISCUSSION

High-Throughput Reaction Screening. Given the large number of palladium catalysts reported for carbonylation reactions⁵ and the anticipated challenges associated with achieving chemoselective carbonylation of β -chloro enones,¹⁵ we began by evaluating eight electrophiles with various functional groups (1a–8a) in a “parallel-in-parallel” screening format (Figure 1).¹⁶ We screened six simple phosphine ligands (PCy₃, P(*t*-Bu)₃, P(Me)(*t*-Bu)₂, dppp, DPEphos, and dcpp) that have either been reported for carbonylation reactivity or is a close analogue (such as P(Me)(*t*-Bu)₂ as a replacement for CataCXium A).¹⁷ We also chose to use the phosphonium tetrafluoroborate salts¹⁸ for all trialkylphosphines in order to ensure reproducibility on a small scale and to simplify automated solid dispensing. In addition to ligand diversity, we also evaluated two bases (triethylamine and

potassium carbonate) and two solvents (acetonitrile and toluene); the other reaction parameters (time, temperature, and CO pressure) were fixed. These reactions were conducted in plates using an HEL Cat96 high-throughput pressure reactor, enabling rapid execution of nearly 200 experiments. Each run was performed using an internal standard (biphenyl), which doubles as both an HPLC and an NMR handle for quantification of the remaining starting material and the desired product.¹⁹ The output of this parallel-in-parallel screen is depicted graphically in Figure 1.

While it is clear from the data that each substrate behaves differently, there are options for a general set of conditions. Both 1a and 2a work well with nearly every ligand tested under multiple base/solvent combinations, while α -substituted chloro enones (3a–8a) are less reactive. For the most sterically demanding substrates, dcpp,^{7k,1} and P(Me)(*t*-Bu)₂ are more effective. In addition, there are clear solvent and base effects on reactivity: CH₃CN and K₂CO₃ generally give higher conversion but also greater byproduct formation. In particular, formation of the corresponding carboxylic acid is enhanced using CH₃CN and/or K₂CO₃, undoubtedly due to adventitious water originating from these hygroscopic materials.

Across this 192-experiment array, the most general system is P(Me)(*t*-Bu)₂ with NEt₃ in either CH₃CN or toluene. These conditions are tolerant of all the assessed functional groups and are even able to achieve chemoselective carbonylation of 8a. While dcpp, dppp, DPEphos, and P(*t*-Bu)₃ all result in mixtures of carbonylation at both Cl and Br (observed by LCMS), P(Me)(*t*-Bu)₂ gives good selectivity for carbonylation at only Cl versus at both Cl and Br (~5:1 desired to overreacted).¹⁹ This is, to the best of our knowledge, the first example of a synthetically useful chemoselective carbonylation of a C(sp²)–Cl over a C(sp²)–Br bond.^{17d,20} These results highlight the power of multivariate screening for reaction optimization: screening only one of these substrates in a univariate manner would not have revealed a general system or yield alternatives specific to each substrate (e.g., dcpp for 3a, PCy₃ for 7a and 8a).

Carbonylation Scope and Preparative-Scale Syntheses. After identifying a general set of conditions for carbonylation of 1a–8a with methanol, we tested these conditions against an array of 80 substrate combinations on a 0.1 mmol scale. Ten functionalized alcohols with varying steric and electronic properties (b–k) were paired with 1a–8a (Figure 2). This set includes a number of challenging alcohol substrates (*tert*-butyl alcohol, trifluoroethanol, phenol, 2-(2-pyridyl)-ethanol), as well as water, which could hydrolyze the chloro enone substrates back to the 1,3-diones. This array was run in a plate-based format analogous to the screen from Figure 1, with products identified by LCMS and assessed semiquantitatively using LC area percent values;¹⁹ 16 examples were further analyzed by ¹H NMR spectroscopy to confirm solution yields, which are in good agreement with the LC area percent values. Across these 80 examples, there is remarkable consistency in product formation using different alcohols, regardless of nucleophilicity or sterics. Water does not seem to hydrolyze the starting materials, allowing access to carboxylic acids in addition to esters. Only substrates 5a and 8a exhibit low conversions in some cases, especially with sterically hindered alcohols. Menthol, one such hindered alcohol, can be used to install an inexpensive chiral auxiliary.^{10b} Even potentially chelating alcohols such as h and k are effective coupling partners, giving highly functionalized ester products in good yields. Finally,

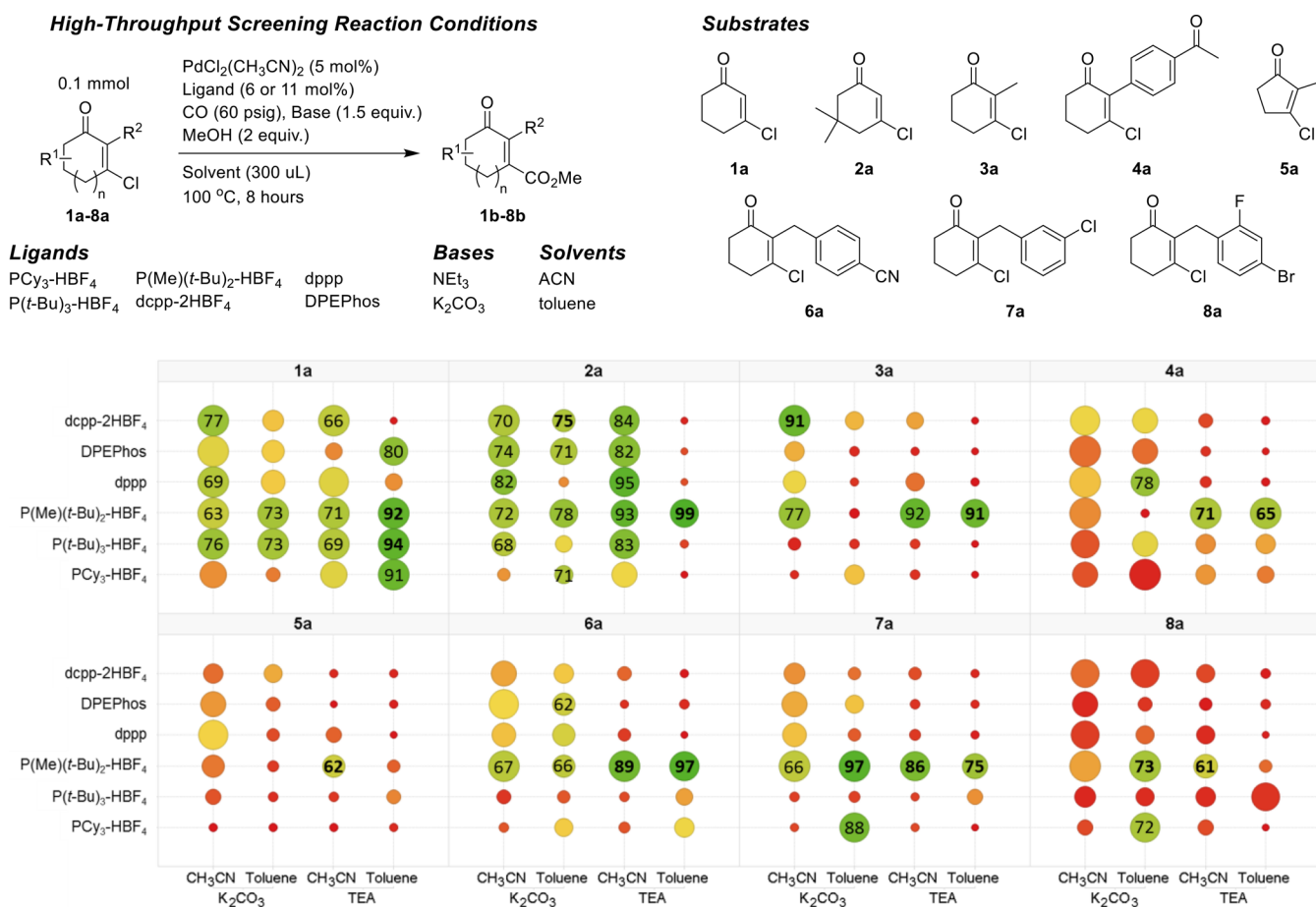


Figure 1. “Parallel-in-parallel” screening design and results. For data visualization, increasing size indicates higher substrate conversion; the color gradient indicates the HPLC solution yield (red, 0%; yellow, 50%; green, 100%). Numbers correspond to solution yields (>60%) determined by HPLC or ¹H NMR spectroscopy (bold values) versus internal standard. See the Supporting Information for a full table of results.

both **7a** and **8a** exhibit chemoselectivity for carbonylation at the vinyl–Cl over the other Ar–X positions.

Twenty examples have been prepared on a gram scale to establish the practical utility of this methodology for a number of challenging substrate combinations (Figure 3). These reactions were conducted at higher concentration with intense mixing, enabling a reduction in both catalyst loading (2 mol %) and temperature (80 °C). Reactions were run under identical conditions (except for carbonylation of **8a**) to enable direct comparisons for the most general set of reaction conditions. Despite being unoptimized, the isolated yields range from 44 to 88%, correlating well with solution yields from screening reactions. In some cases, we observe small amounts of alkene isomerization in the crude ¹H NMR spectra; however, these isomeric byproducts are removed during chromatographic purification.¹⁹ One exception is the acetophenone-substituted ester **4b**, which was isolated as an inseparable 2.3:1 mixture of alkene isomers. For reactions with **8a**, we observed only ~10% carbonylation at Br to give the diester byproduct; no evidence for carbonylation at only Br to give a monoester byproduct was observed.¹⁹

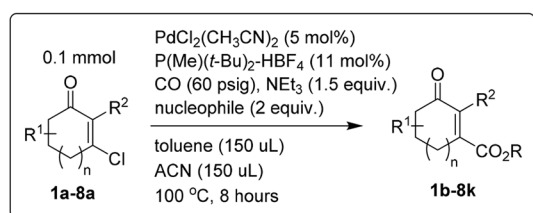
We have also monitored several of these reactions over time by liquid sampling using an Unchained Laboratories OSR apparatus,²¹ revealing a wide range of rates for different substrate combinations (Figure 4). Comparing the rates of carboxylic acid formation for **1c**, **3c**, **5c**, or **6c** indicates that the steric properties of the electrophile have a large effect on rate, with

the reactivity order **1a** > **3a** ≈ **6a** > **5a**. Similarly, increasing nucleophile steric bulk leads to diminished rates, as observed for the formation of **1c,f,g**.

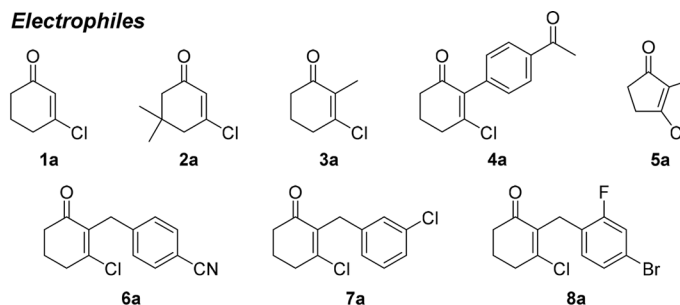
While the conditions from Figure 3 are a valuable starting point for exploratory synthesis, we emphasize that the listed yields are unoptimized and can certainly be improved with further development. For example, during process optimization for the production of **1b**, which is commercially available in small quantities with inconsistent quality, we re-evaluated $\text{P}(t\text{-Bu})_3$ as a ligand due to its greater availability on a large scale. Reaction monitoring using the OSR revealed that the formation of **1b** proceeds to 80–90% in ~30 min, even at catalyst loadings ≤1 mol %. In fact, these results revealed an apparent zero-order dependence on catalyst concentration, leading us to suspect mass transfer as contributing to the rate.¹⁹ Obtaining meaningful kinetic data under synthetically relevant conditions proved extremely difficult, which prompted an exploration of stoichiometric reactivity as an alternative means to study the potential reaction mechanisms for the formation of **1b** using $\text{P}(t\text{-Bu})_3$.

Stoichiometric Reactivity and Isolation of Pd(II) Vinyl and Acyl Species. The high reactivity of β -chloro enones toward carbonylation is in stark contrast to difficult carbonylations of other $\text{C}(\text{sp}^2)\text{-Cl}$ substrates.^{7,17d} As slow oxidative addition of the C–Cl bond is often blamed for poor reactivity of aryl and vinyl chlorides in Pd-catalyzed carbonylation,⁷ we targeted our stoichiometric studies toward this reaction

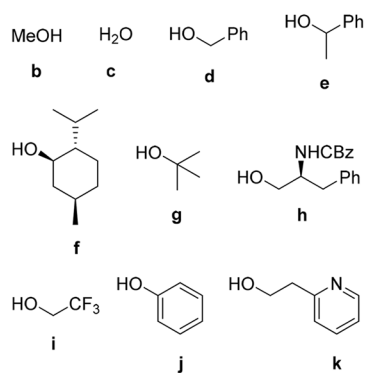
Reaction Scope Evaluation



Electrophiles



Nucleophiles



	1	2	3	4	5	6	7	8
b	79	78	67	57	46	89	90	33
c	75	77	82	65	49	87	97	66
d	83	93	79	77	87	88	88	61
e	72	79	80	71	63	94	90	63
f	80	84	82	76	44	84	90	•
g	74	75	47	50	37	84	92	•
h	80	87	90	79	88	87	89	62
i	58	83	95	75	91	83	71	62
j	67	75	84	59	91	88	76	68
k	53	66	53	44	42	70	89	46

Figure 2. Plate-based reaction scope evaluation between **1a–8a** and **b–k** under one set of reaction conditions. For data visualization, increasing size corresponds higher substrate conversion; the color gradient indicates the solution yield of the desired product (red, 0%; yellow, 50%; green, 100%). Numbers correspond to solution yields (>30%) determined by HPLC or ^1H NMR spectroscopy (boldface values) versus internal standard. See the [Supporting Information](#) for a full table of results.

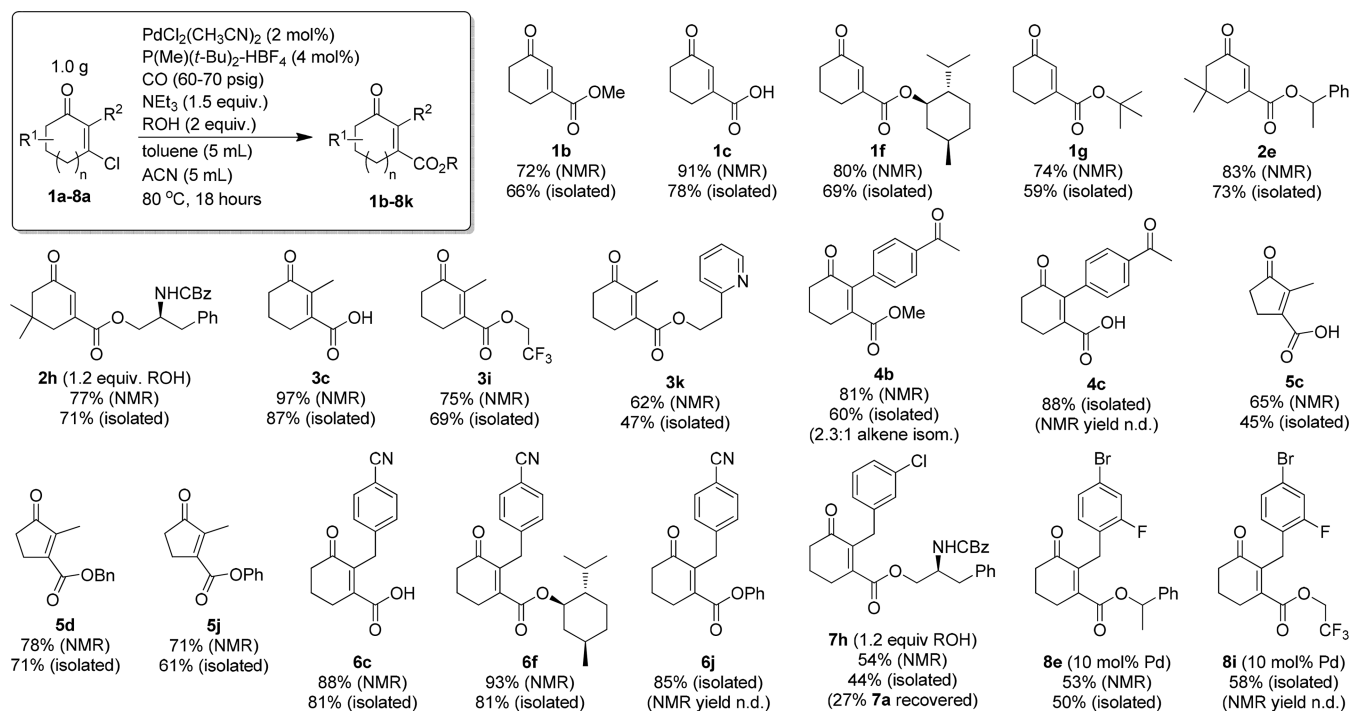


Figure 3. Gram-scale synthesis of 20 γ -keto esters and acids with solution (NMR) and isolated yields.

(Scheme 2). Monitoring the reaction of a 1:1 mixture of $\text{Pd}[\text{P}(t\text{-Bu})_3]_2$ and **1a** at 60 °C for 1 h reveals ~10% of a new species, which we propose is the oxidative addition complex **9**,

along with ~10% of free $\text{P}(t\text{-Bu})_3$ (Scheme 2A). Unfortunately, prolonged heating does not give an increase in **9** but rather formation of multiple new Pd species (observed by ^31P

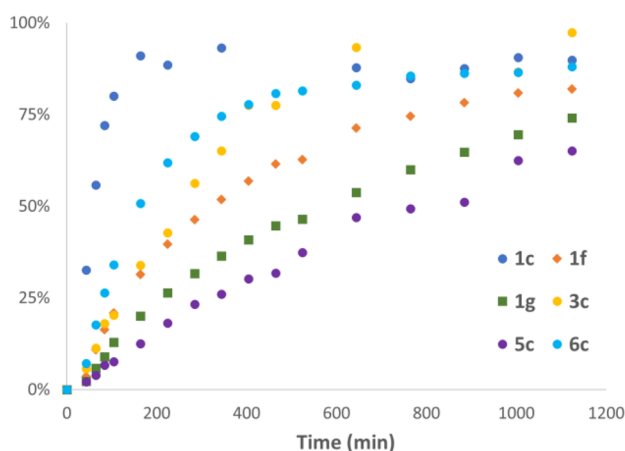


Figure 4. Reaction progress plots for selected examples.

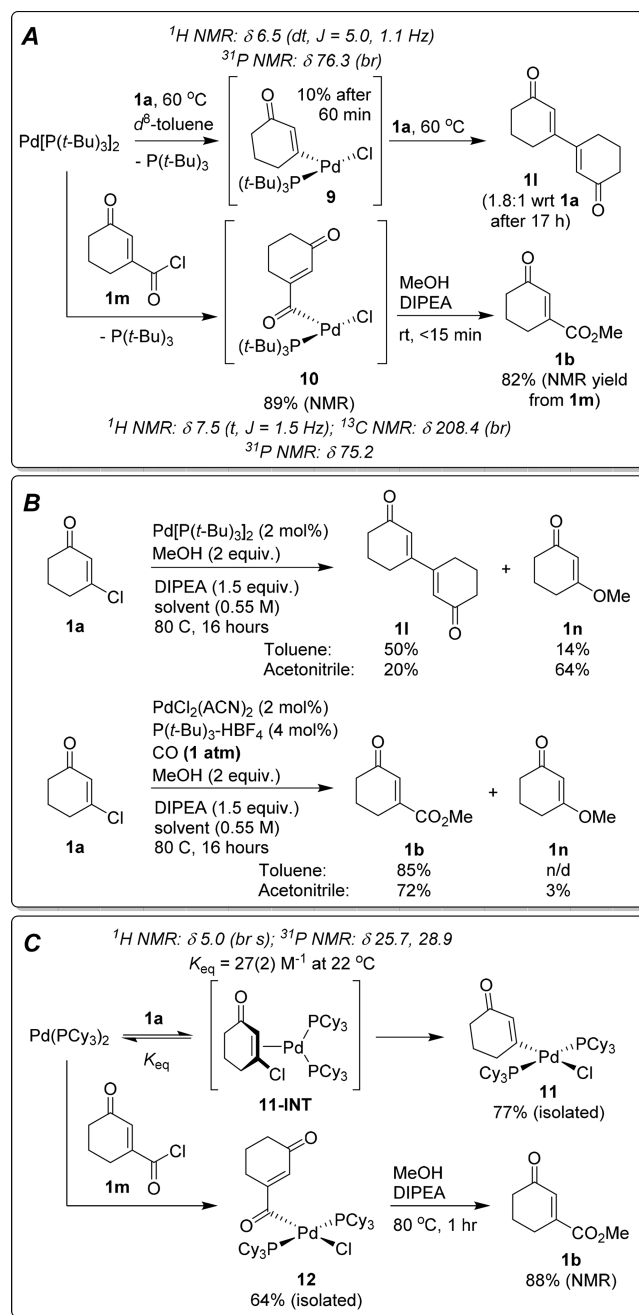
NMR spectroscopy) and concomitant reductive homocoupling of the cyclohexenone moiety to give **11**. After heating for 17 h at 60–70 °C, there is an approximately 2:1 ratio of **11** to **1a**, with only minimal **9** present.

We attribute the minimal formation of **9** under these conditions to the fact that oxidative addition to Pd[P(*t*-Bu)₃]₂ proceeds via the monophosphine complex after dissociation of 1 equiv of P(*t*-Bu)₃.²² As the reaction progresses, buildup of free P(*t*-Bu)₃ will disfavor phosphine dissociation from Pd[P(*t*-Bu)₃]₂, limiting the rate of oxidative addition. Subsequent decomposition to **11** may occur via migratory insertion of the Pd–C bond onto the alkene of another equivalent of **1a**, followed by β-chloride elimination (effectively a reductive Heck coupling) or via disproportionation of **9** to generate a bis(vinyl) palladium species and Pd[P(*t*-Bu)₃]₂Cl₂, followed by reductive elimination of **11**.

Generation of the corresponding acyl complex (**10**) was accomplished by reacting Pd[P(*t*-Bu)₃]₂ with the acid chloride **1m**. Rapid conversion to **10** (89% solution yield vs internal standard) and 1 equiv of free P(*t*-Bu)₃ is observed at room temperature. The ¹H NMR spectrum of complex **10** has a diagnostic downfield singlet (7.5 ppm) for the vinyl C–H; a broad downfield ¹³C NMR signal at 208.5 ppm is indicative of a Pd–acyl unit. Unfortunately, attempts to isolate **10** have not been successful. While **10** can be precipitated from toluene/pentane in 50–60% yield, this material is not pure and completely decomposes in solution after 24 h at room temperature, forming a complex mixture that includes **11**. In this case, formation of **11** must occur via decarbonylation²³ to give **9**, followed by disproportionation; a Heck-type pathway cannot be operative, as **1a** is not present. Thus, we favor disproportionation as the likely mechanism for formation of **11** in our attempts to prepare **9** from **1a** and Pd[P(*t*-Bu)₃]₂ but cannot completely rule out the Heck-type pathway. Finally, treatment of **10** with excess MeOH and DIPEA directly generates **1b** in 82% solution yield at room temperature in <15 min.

Observation of reductive homocoupling in stoichiometric reactions with P(*t*-Bu)₃ led us to investigate its relevance under catalytic conditions (Scheme 2B). In the absence of CO, both **11** and the direct substitution product **1n** are formed, with the product distribution dependent on the reaction solvent. This indicates that MeOH can act both as a nucleophile and as a reductant to effect catalytic turnover in the formation of **11**. To assess whether low *p*_{CO} could result in either **11** or **1n** as byproducts in the carbonylation of **1a**, we performed this

Scheme 2. Formation of Vinyl and Acyl Pd Species and Observation of Byproducts during Catalysis with 0–1 atm of CO



transformation with only 1 atm of CO, leading to an 85% or 72% solution yield of **1b** in toluene or acetonitrile, respectively. While 3% of **1n** is observed using acetonitrile, we do not observe evidence for **11** in either solvent. Despite the absence of **11** from these catalytic runs at 1 atm of CO, formation of **11** and/or **1n** is a possible failure mode if insufficient CO is present. As a result, we have maintained at least 60 psi of CO in our preparative-scale carbonylation processes.

In an effort to cleanly isolate a Pd–vinyl species derived from oxidative addition of **1a**, we explored the reactivity of Pd(PCy₃)₂ under analogous conditions. While PCy₃ is by no means the most reactive ligand in the carbonylation chemistry, it is active for carbonylation of **1a** to **1b** (Figure 1). Pd(PCy₃)₂

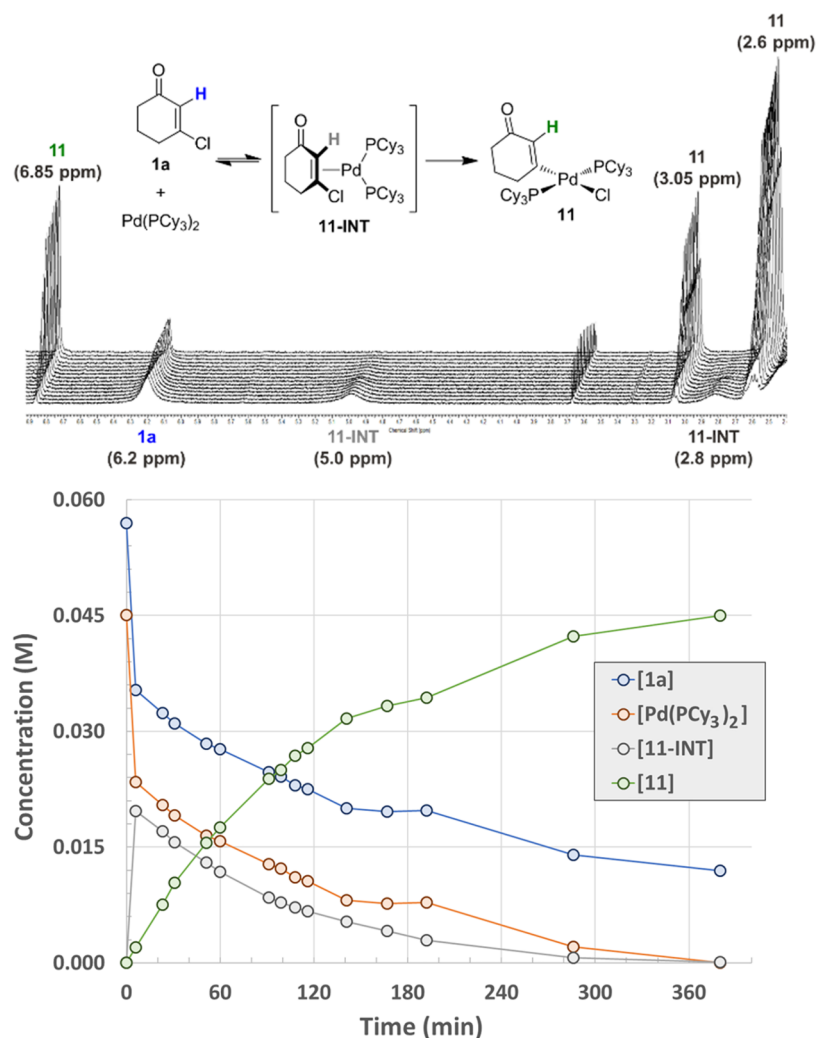


Figure 5. (top) Stack plot of ¹H NMR spectra (2.4–6.9 ppm) acquired over time during the oxidative addition of **1a** to Pd(PCy₃)₂ (time increases front to back). (bottom) Reaction progress plot (concentrations determined by integration versus biphenyl as an internal standard or, in the case of Pd(PCy₃)₂, calculated assuming mass balance).

is known to undergo direct oxidative addition without phosphine dissociation,²⁴ which we anticipated would mitigate the conversion problem observed for Pd[P(*t*-Bu)₃]₂. Finally, Pd(PCy₃)₂ is readily available in pure form (unlike Pd[P-(Me)(*t*-Bu)₂]₂, which cannot be crystallized and is typically generated in situ²⁵).

Treating Pd(PCy₃)₂ with **1a** results in smooth formation of the desired complex (**11**) (Scheme 2C), which has been isolated (77% yield) and fully characterized. Monitoring the oxidative addition reaction progress by both ¹H and ³¹P NMR spectroscopy reveals the presence of an intermediate that we have assigned as the alkene complex (**11-INT**) on the basis of diagnostic signals in the ¹H and ³¹P NMR spectra.^{19,26} This intermediate forms upon mixing and then completely converts to complex **11** over 6 h (Figure 5). In addition, we observe broad peaks for the vinyl C–H signal of **1a** and **11-INT**; a 2D ROESY NMR spectrum confirms exchange between free and coordinated **1a** on the NMR time scale.¹⁹ Calculating *K*_{eq} for alkene coordination from the concentrations of **1a**, Pd(PCy₃)₂, and **11-INT** determined in the first 3 h of the reaction gives a value of 27(2) M⁻¹ at room temperature.

Reacting Pd(PCy₃)₂ with the acid chloride **1m** results in rapid oxidative addition to the Pd–acyl complex **12**, which has

been isolated in 64% yield by precipitation from heptane. Unlike **10**, this acyl species is stable upon isolation, undoubtedly because it is coordinatively and electronically saturated. The NMR spectroscopic features of **12** are consistent with those observed for **10**, with downfield resonances in both the ¹H (8.0 ppm for the vinyl C–H) and ¹³C (240.5 ppm for the Pd–acyl carbon) NMR spectra. This species can also be generated by subjecting **11** to a CO atmosphere at 80 °C for 1 h, giving a 1.4:1 mixture of **11** and **12**; prolonged heating results in decomposition. As for complex **10**, treatment of **12** with excess MeOH and DIPEA generates **1b** (88% solution yield); however, rather than being complete in minutes at room temperature, ester formation from **11** requires more forcing conditions (80 °C, 1 h).

Single crystals of complexes **11** and **12** have been analyzed by X-ray crystallography to establish the solid-state molecular structures; the ORTEP drawings are shown in Figure 6, along with key bond lengths and angles in Table 1. Complex **11** is essentially isostructural with Pd(PCy₃)₂(Ph)Cl,^{7a} with the phosphine ligands situated trans in a slightly distorted square planar geometry. The cyclohexenyl group is orthogonal to the square plane (P1–Pd1–C1–C2 torsion angle: 95°), with a Pd–C distance of slightly less than 2.0 Å. Complex **12** has

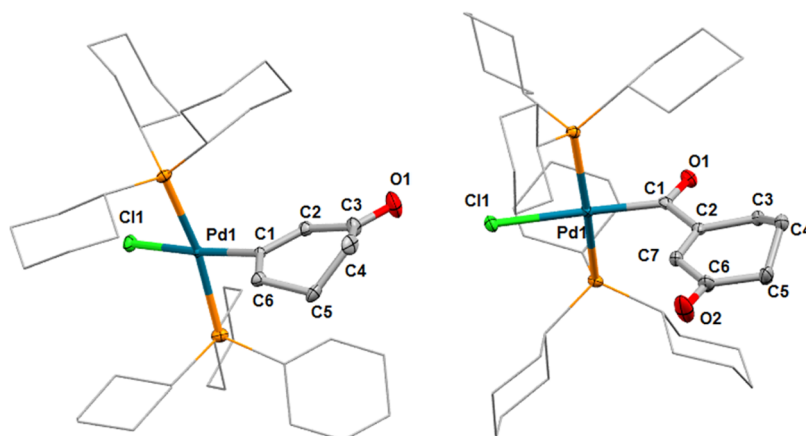


Figure 6. ORTEP representations of the solid-state molecular structures of complexes **11** (left) and **12** (right) determined by X-ray crystallography. Thermal ellipsoids are plotted at 50% probability; phosphine substituents are displayed as wireframe for clarity. Complex **11** has a plane of symmetry through the Cl1–Pd1–C1 plane, rendering both PCy₃ ligands equivalent, and C5 is disordered over two positions (one shown for clarity). Complex **12** crystallizes with two inequivalent molecules in the asymmetric unit; the image and metrical parameters correspond to one of these molecules.

Table 1. Bond Lengths (Å), Bond Angles (deg), and Torsion Angles (deg) for Complexes **11** and **12**

	complex 11		complex 12
Pd1–C1	1.988(7)	Pd1–C1	1.9827(18)
Pd1–P1	2.3540(11)	Pd1–P1	2.3812(5)
		Pd1–P2	2.3581(5)
Pd1–Cl1	2.4147(18)	Pd1–Cl1	2.4302(5)
		C1–O1	1.212(2)
		C1–C2	1.526(3)
C1–C2	1.380(9)	C2–C7	1.335(3)
C2–C3	1.455(10)	C6–C7	1.474(3)
C3–O1	1.230(10)	C6–O2	1.219(3)
C3–C4	1.525(12)	C5–C6	1.508(3)
C1–Pd1–Cl1	172.3(2)	C1–Pd1–Cl1	178.02(6)
P1–Pd1–P1	169.71(7)	P1–Pd1–P2	169.846(18)
C1–Pd1–P1	91.31(4)	C1–Pd1–P1	94.26(5)
		C1–Pd1–P2	88.03(5)
Cl1–Pd1–P1	89.37(4)	Cl1–Pd1–P1	86.050(16)
		Cl1–Pd1–P2	92.008(16)
P1–Pd1–C1–C2	95.0(2)	P1–Pd1–C1–O1	88.6(2)

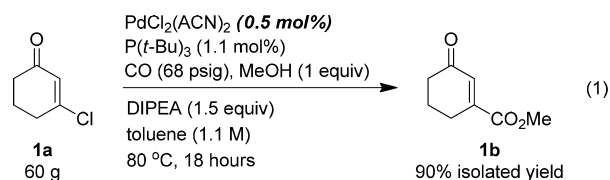
essentially the same structural features, with the acyl ligand oriented orthogonal to the square plane and a similar Pd–C distance of 1.98 Å.

While further kinetic and spectroscopic studies under the carbonylation reaction conditions are required to fully elucidate the catalytic mechanism, the stoichiometric chemistry from **Scheme 2** points to key differences in reactivity depending on ligand identity. As documented for oxidative addition of aryl halides, Pd/P(*t*-Bu)₃ and Pd/PCy₃ systems undergo oxidative addition with **1a** via dissociative²² or associative²⁴ mechanisms, respectively. Precoordination of the alkene to Pd(PCy₃)₂ is rapid and favorable (on/off rates on the NMR time scale, with $K_{eq} = 27 \text{ M}^{-1}$), whereas the need for phosphine dissociation from Pd[P(*t*-Bu)₃]₂ limits the extent of oxidative addition under stoichiometric conditions.

On the other hand, methanolysis of the P(*t*-Bu)₃-ligated acyl complex **10** is rapid, reaching complete conversion in minutes even at room temperature. This is in stark contrast to the reactivity of PCy₃-ligated acyl complex **12**, where methanolysis

requires 1 h at elevated temperature. These rate differences are almost certainly due to the coordination environments of the two acyl species. Complex **12** is coordinatively and electronically saturated, meaning that PCy₃ dissociation is likely required for methanolysis to occur. In contrast, complex **10** has an open coordination site to accommodate the incoming nucleophile. Of course, the presence of CO will lead to changes in Pd speciation and the rates of elementary steps in the catalytic cycle; kinetic studies to probe these aspects are ongoing.

Large-Scale Preparation of 1b. All of the information gathered during screening, gram-scale preparations, and stoichiometric organometallic studies has informed our development of a multigram preparation of **1b**. Given the very fast rates observed for the formation of **1b** using P(*t*-Bu)₃ even at low catalyst loadings, we chose this ligand over P(Me)(*t*-Bu)₂ for further development; large-scale availability was also a consideration. On the basis of the results shown in **Scheme 2B**, we chose toluene as the reaction solvent, limited the MeOH charge to 1 equiv, and maintained an elevated CO pressure (eq 1). Another key aspect of the reaction setup is to charge



CO at room temperature, followed by heating to 80 °C, rather than the more typical reverse order of operations. All of these choices were made to minimize or eliminate the formation of **11** and **1n**. Furthermore, moving to a single solvent system rather than the mixed toluene/acetonitrile conditions from **Figure 3** simplifies the process considerably and makes solvent recycling on a commercial scale more feasible. Finally, we increased the reaction concentration to >1 M in **1a** to maximize volume efficiency.

Our initial 60 g scale run with 1.3 mol % of Pd reached completion in only 20 min as judged by CO uptake, enabling a further reduction in catalyst loading. Using only 0.5 mol % of Pd gives **1b** in 90% isolated yield (eq 1). Analysis of the crude product by both NMR and LCMS indicates a very high level of

purity after only a simple aqueous workup, with residual catalyst as the only significant contaminant. We believe that carbonylation of β -chloro enones will now be a preferred method to prepare structurally varied cyclic γ -keto ester and acid derivatives on scale.

CONCLUSIONS

By employing high-throughput screening of multiple substrates simultaneously, we have developed a general, operationally simple, and scalable synthesis of cyclic α,β -unsaturated γ -keto esters and acids via the Pd-catalyzed carbonylation of easily accessed β -chloro enones. Using an appropriate catalyst system, centered on simple trialkylphosphine ligands such as $P(\text{Me})(t\text{-Bu})_2$ and $P(t\text{-Bu})_3$, enables carbonylative coupling between a wide array of functionalized electrophiles and oxygen-based nucleophiles with exceptional chemoselectivity. These reactions can be carried out at high reaction concentrations on a multigram scale, providing rapid and efficient access to these versatile compounds.^{8–12} We believe a key element of the carbonylation reactivity observed is coordination of the enone $\text{C}=\text{C}$ bond to Pd prior to oxidative addition, combined with the high electrophilicity of the β -carbon. This propensity of β -chloro enones to add to Pd(0) will likely find application in many other cross-coupling reactions under mild conditions,²⁷ especially given that the chloro enone moiety can be functionalized in the presence of many other potentially sensitive groups. Evidently, a chloro enone can be more activated toward oxidative addition in comparison to an aryl bromide—when an appropriate ligand is used—enabling chemoselective functionalization. Further studies on elucidating the reaction scope and mechanism are currently underway and will be reported in due course.

EXPERIMENTAL SECTION

General Information. All common reagents and solvents were purchased from commercial sources and used as received. Palladium catalysts and ligands were stored and handled under dry nitrogen in gloveboxes unless otherwise noted. $\text{Pd}[\text{P}(t\text{-Bu})_3]_2$ and $\text{Pd}(\text{PCy}_3)_2$ were obtained from Strem and stored at -35°C in a glovebox. All chloroenone substrates were stored at -20°C to prevent decomposition, which appears to occur via hydrolysis back to the corresponding dione.

Analytical Details. All NMR spectra were acquired at ambient temperature on a Bruker 400 MHz spectrometer. Solvents and frequencies for specific data acquisitions are noted for each case in the following sections. Chemical shifts were calibrated relative to residual protio solvent (^1H and ^{13}C) or to external standards (^{31}P and ^{19}F). Data were processed using TopSpin and reports generated using ACD SpecManager.

HPLC analysis was performed on Agilent 1260 or 1290 series instruments with diode array detectors, though analysis was typically done with traces from a single wavelength. Two HPLC methods were utilized during the course of this work. Method A (1260 series): column, Zorbax SB-C18, 1.8 μm , 3×50 mm; column temperature, 60°C ; flow rate, 1.5 mL/min; solvent gradient, ACN (0.05% TFA v/v)/ H_2O (0.05% TFA v/v), from 100/0 to 5/95 over 2.7 min; detection wavelength, 220 nm. Method B (1290 series): column, Waters X-Select CSH, 2.5 μm , 2.1×30 mm; column temperature, 45°C ; flow rate, 1.6 mL/min; solvent gradient, ACN (0.05% TFA v/v)/ H_2O (0.05% TFA v/v), from 97/3 to 5/95 over 1.9 min; detection wavelength, 220 nm.

LCMS analysis was performed on a Waters Acquity system equipped with UV (Waters Acquity PDA, 210–360 nm), ELS (Waters Acquity ELSD, 50°C), and MS (ESI, Waters Acquity SQD, positive ion mode, scan time 0.1 s) detectors. Chromatography method: column, Waters CSH (C18), 1.7 μm , 2.1×30 mm; column

temperature, 45°C ; flow rate, 1.3 mL/min; solvent gradient, ACN (0.05% TFA v/v)/ H_2O (0.05% TFA v/v), from 97/3 to 2/98 over 1.9 min.

SAFETY NOTE. Pressurized carbonylation reactions should always be carried out in well-maintained, leak-checked pressure equipment located in a well-ventilated environment, preferably a dedicated pressure laboratory. Carbon monoxide detectors should always be in use and a buddy system employed to ensure safe operation. Before any large-scale reaction (>100 g input) is performed, a thorough safety assessment should be conducted, including reaction calorimetry studies.

General Procedures for High-Throughput Screening. Plate Setup. Small-scale HTS reactions were carried out on 0.10 mmol scale with a total reaction volume of ~ 0.3 – 0.4 mL. Solid bases, palladium sources, and ligands were automatically dosed using a Quantos QX96 (Mettler Toledo) instrument housed inside a nitrogen glovebox. These materials were dispensed into a 48-well array of 1.5 mL crimp-cap HPLC vials containing micro stirbars. The plate was removed from the glovebox, and all liquid reagents and stock solutions of substrates/biphenyl (internal standard) in reaction solvent were dispensed via micropipet to the appropriate vials according to the experimental design on the benchtop.

Reaction. Once all materials were charged, each vial was sealed with an aluminum crimp-cap containing a PTFE/silicone/PTFE septum. The septa were pierced with a wide-bore needle to allow gas ingress/egress. The vials (arrayed in a metal plate) were heated to the desired reaction temperature with magnetic stirring under the desired pressure of carbon monoxide (~ 60 psig) inside a Cat96 pressure reactor (HEL). Prior to the commencement of heating/stirring, the following purge cycles were conducted: 3×75 psig nitrogen, 3×70 psig carbon monoxide. At the end of the desired reaction time, stirring was stopped, the reactor was cooled to room temperature, and the atmosphere was replaced with nitrogen following 3×5 bar purge cycles.

Analysis. Once the system returned to ambient pressure, the plate was removed and the caps were removed. Each vial was diluted with 0.7 mL of acetonitrile. The plate was placed on a stirplate to ensure complete dissolution of any organic products. The resulting suspensions were centrifuged prior to withdrawing 20 μL aliquots via micropipet. These aliquots were diluted into an analysis plate with wells containing 1 mL of acetonitrile. The analysis plate was then analyzed by either HPLC or LCMS to assay for desired product and the remaining starting material. Select reactions were also analyzed by ^1H NMR to obtain solution yields versus internal standard (biphenyl).¹⁹

General Procedures for Gram-Scale Carbonylation Reactions. Gram-scale runs were performed using either an HEL AutoMATE parallel pressure reactor with 50 mL vessels and magnetically driven stirring with a fixed magnetic impeller or using an Unchained Laboratories OSR unit with 30 mL vessels and overhead mechanical stirring. General procedures for the reaction setup in each reactor type, as well as the general workup and isolation, are described below.

HEL AutoMATE. The entirety of this preparation was carried out on the benchtop. The desired electrophile (1 g) and biphenyl (internal standard) were dissolved in 5 mL of anhydrous toluene in a scintillation vial, and the desired nucleophile (2 equiv, except for runs with **h**, where 1.2 equiv was used) was dissolved in anhydrous acetonitrile (5 mL) in a second vial. A 50 mL Hastelloy reactor bottom was staged in the AutoMATE deck and charged with solid $\text{PdCl}_2(\text{ACN})_2$ (2 mol %, or 10 mol % with **8a**) and $\text{P}(\text{Me})(t\text{-Bu})_2\text{-HBF}_4$ (4 mol %, or 20 mol % with **8a**). In quick succession, the toluene solution of substrate/standard, triethylamine (1.5 equiv), and the acetonitrile solution of the nucleophile were added to the catalyst solids via syringe. Note that this order of addition is critical to reaction success: adding the nucleophile prior to the triethylamine can result in substrate and/or catalyst decomposition. Once the solutions were charged, the vessel was screwed into the reactor top and lowered into the heat well. Stirring was commenced, and the reactor was pressurized with 60 psig of nitrogen and vented three times. The reactor

was then pressurized with 60 psig of carbon monoxide, vented three times, and pressurized back to 60 psig of carbon monoxide. The reactor was heated to 80 °C for 18 h with stirring at 450 rpm and was set to maintain a minimum pressure of 70 psig throughout the reaction. After 18 h, stirring was stopped and the vessel cooled to room temperature. After 1 h, the reactor was vented and the headspace replaced with 60 psig of nitrogen. Finally, before the reaction mixture was retrieved, the reactor was vented.

Unchained Laboratories OSR. This procedure was used to prepare compounds **1c**, **f**, **g**, **3c**, **5c**, and **6c**. The entirety of this preparation was carried out inside a nitrogen glovebox. A 30 mL OSR glass liner was charged with solid PdCl₂(ACN)₂ (2 mol %) and P(Me)₃(tBu)₂-HBF₄ (4 mol %). The desired electrophile (1 g) and biphenyl (internal standard) were dissolved in 5 mL of anhydrous toluene in a scintillation vial and then transferred to the catalyst solids. Triethylamine (1.5 equiv) was added, followed by the desired nucleophile (2 equiv) dissolved in anhydrous acetonitrile (5 mL). Note that this order of addition is critical to reaction success: adding the nucleophile prior to the triethylamine can result in substrate and/or catalyst decomposition. Once the solutions were charged, the liner was placed in the OSR module and the reactor top was fixed in place. Each step in the process was predefined in a library design made with Unchained Laboratories Library Studio software and executed with Automation Studio software. The stirring rate was set to 500 rpm followed by purging of the reactors with ~120 psig of nitrogen and subsequently 100 psig of carbon monoxide. The pressure was then set to the operating pressure of 60 psig, which the system automatically refills after the pressure level falls under 55 psig. An initial sample was then taken (corresponding to $t = 0$). All samples taken were deposited directly in 1.5 mL HPLC sample vials in a 48-well plate orientation. The reactor top, which also contains the stirring belt, was set to 95 °C; this temperature is above the reactor operating temperature to prevent reflux in the vessel. Once the reactor top was at temperature, each reactor was brought to temperature (80 °C) with a 3 min delay to account for sampling time (each sampling cycle is 3 min). Sampling then occurred every 15 min for the first 1 h, every 1 h for hours 1–8, and every 2 h for hours 8–18 (17 total samples from each reactor) followed by dilution with acetonitrile. After the final time point was sampled at 18 h, the reactors were vented and cooled to room temperature. After the reactors cooled, the reactor top was removed and glass liners removed for further isolation and characterization. Samples taken were moved directly to HPLC for analysis.

Workup and Isolation. The crude reaction mixture was diluted with TBME (10 mL) or ethyl acetate (10 mL, for carboxylic acid products), brine (8 mL), and 1 M HCl (8 mL) to completely dissolve all solids (HNEt₃Cl), followed by transfer to a separatory funnel. The phases were well mixed, and then the aqueous layer was removed. The aqueous layer was back-extracted with TBME (10 mL) or ethyl acetate (10 mL, for carboxylic acid products), and the combined organic phases were dried over MgSO₄. After filtration, the solvent was removed in vacuo, and a ¹H NMR spectrum was obtained of the crude material to determine an NMR yield. For all ester products (except **3k**), the residue was redissolved in 10–20 mL of hexanes (using a minimum amount of EtOAc if required) and purified by column chromatography with either a 0–20% or 0–40% ethyl acetate in hexanes gradient, depending on the R_f value for the desired product (determined by TLC). All preparative column chromatography was performed using a Teledyne ISCO Combiflash R_f system with prepacked RediSep columns.

Carboxylic acid products were not subject to chromatography but were purified in the following manner. The crude residue was dissolved in a mixture of TBME (20 mL) and 1 M NaOH (20 mL) with vigorous mixing. After mixing, the layers were allowed to settle and then separated. The aqueous layer was back-extracted with TBME (10 mL). The basic aqueous layer was then acidified with 3 M HCl to pH <2 before extraction with ethyl acetate (3 × 10 mL). The combined ethyl acetate layers were dried over MgSO₄, filtered, and concentrated in vacuo to give the carboxylic acid products as white/off-white solids.

Compound **3k** was purified by selective extractions.¹⁹

Large-Scale Preparation of 1b. Procedure. A 1 L Buchiglas Ecolave pressure reactor equipped with an overhead stirrer and a gas inlet controlled by a mass-flow controller was flushed with nitrogen. The nitrogen stream was maintained throughout the reaction setup. The reactor was rinsed with anhydrous toluene (3×) prior to charging reagents. 3-Chlorocyclohex-2-enone (**1a**; 60.0 g, 460 mmol) was dissolved in anhydrous toluene (250 mL) and added to the reactor. Stirring was commenced at 700 rpm. Solid PdCl₂(ACN)₂ (0.600 g, 2.31 mmol) was charged through an addition port using a powder funnel. The funnel was rinsed with a small amount of toluene to ensure a quantitative transfer. The addition port was fitted with a rubber septum, and the system was vented through a second port. Tri-*tert*-butylphosphine (1.00 g, 4.94 mmol) was dissolved in anhydrous toluene (50 mL) inside a nitrogen glovebox. This solution was drawn into a large syringe, which was brought out of the glovebox to the pressure reactor. The ligand solution was added to the reactor through the septum. DIPEA (89.0 g, 120 mL, 689 mmol) was added via syringe through the septum, followed by methanol (15.8 g, 20 mL, 494 mmol). The septum was removed and the reactor sealed and the headspace purged with 30 psig of nitrogen three times. Stirring was then stopped, and the headspace was purged with 30 psig of CO three times. The reactor was then pressurized with 68 psig of CO, and the uptake monitor on the mass-flow controller was reset to zero. Stirring was restarted at 1000 rpm, and the reaction mixture was heated to 80 °C over 35 min. Gas uptake commenced once the temperature had surpassed 55 °C. The initial rate of CO uptake was monitored extensively for 20 min after the reaction temperature was reached and then periodically until 180 min.¹⁹ The reaction mixture was stirred under constant CO pressure at 80 °C for 18 h. The next morning, the total CO uptake was observed to be ~460 mmol, indicating reaction completion. The reaction mixture was an orange solution with a suspended gray/white solid. The reaction mixture was cooled to 20 °C over 35 min, followed by depressurization and purging with nitrogen to ensure all CO was removed. An aliquot was analyzed by LCMS, showing >95% area for the desired product and no remaining **1a**.

Workup and Purification. The reaction mixture was drained into a 2 L Erleyemeyer flask via the bottom valve, and the reactor was rinsed three times with a 1/1 toluene/water mixture (300 mL total volume) with stirring to ensure a quantitative transfer. The mixed organic/aqueous phases were transferred to a separatory funnel, and the layers were separated. The organic phase was dried over MgSO₄, and the solvent was removed after filtration to give an orange oil. A ¹H NMR spectrum of the crude product indicated that all DIPEA was removed in the workup. The only other discernible components were a small amount of P(O)(*t*-Bu)₃ and residual toluene. In order to remove the residual palladium, the material was purified by passage through a silica plug as follows. A 3 L medium-porosity glass frit was loaded with 750 g of silica gel (approximate dimensions of the plug: 12 in. diameter, 3 in. depth). The silica was slurried with heptane with stirring using a glass rod to remove air bubbles and inhomogeneities. The heptane was allowed to drain via gravity. Once the solvent level reached the top of the silica bed, the neat orange oil was loaded onto the plug, using heptane to ensure a quantitative transfer. Once the compound was loaded, a 2 in. depth bed of sand was added to the top of the plug, and the desired compound was eluted with a heptane/ethyl acetate mixture (3 L of 10/1 heptane/ethyl acetate, 2 L of 7.5/1 heptane/ethyl acetate, 2 L of 5/1 heptane/ethyl acetate). The eluent solutions were concentrated in vacuo to give pure **1b** (63.8 g, 90% yield).

Synthesis of 11. In a nitrogen-filled glovebox, a tared 4 mL screw-cap vial was charged with Pd(PCy₃)₂ (120 mg, 0.180 mmol) and a stirbar. A second 4 mL vial was charged with **1a** (25.8 mg, 0.198 mmol) and toluene (3 mL). The solution of **1a** was transferred to the vial containing Pd(PCy₃)₂, and the mixture was stirred until it was homogeneous. The stirbar was then removed, and the mixture was left to stand at room temperature over several days to crystallize the product. The mother liquor was then decanted, and the white solid was washed with pentane (2 × 1 mL) and dried in vacuo. The solid was again triturated with pentane to remove residual toluene solvent and dried extensively in vacuo to give compound **11** (110 mg, 77% yield). ¹H NMR (400 MHz, CD₂Cl₂): δ (ppm) 1.10–1.39

(m, 18 H, 18 × Cy-H), 1.51–1.77 (m, 18 H, 18 × Cy-H), 1.77–1.90 (m, 12 H, 12 × Cy-H), 1.90–2.16 (m, 14 H, $-\text{CH}_2\text{CH}_2\text{C}=\text{CH}-$, 12 × Cy-H), 2.32 (m, 8 H, 6 × PCHR₂, $-\text{CH}_2\text{C}=\text{CH}-$), 2.90 (t, *J* = 5.5 Hz, 2 H, $-\text{CH}_2\text{C}=\text{O}$), 6.40 (s, 1 H, $-\text{C}=\text{CH}-$). ¹³C{¹H} NMR (101 MHz, CD₂Cl₂): δ (ppm) 24.53, 26.53, 27.76 (d, *J* = 9.80 Hz), 27.81 (d, *J* = 9.50 Hz), 27.86 (d, *J* = 9.80 Hz), 30.17 (d, *J* = 24.50 Hz), 33.82 (d, *J* = 9.40 Hz), 33.91 (d, *J* = 9.40 Hz), 37.95, 39.53, 136.84 (t, *J* = 2.80 Hz), 191.25, 199.15 (br). ³¹P{¹H} NMR (162 MHz, CD₂Cl₂) δ (ppm) 21.13. LRMS (ESI): obtained using LCMS under standard conditions; fragment observed between *m/z* 760 and 767 in diagnostic isotope pattern, with most intense peak at *m/z* 762, corresponding to [Pd(PCy₃)₂(R)]⁺; another fragment observed between *m/z* 520 and 527 in a diagnostic isotope pattern, with most intense peak at *m/z* 522, corresponding to [Pd(PCy₃)-(CH₃CN)(R)]⁺; final major fragment observed at *m/z* 281 for [HPCy₃]⁺. These isotope patterns are pictured in the Supporting Information. Anal. Calcd for C₄₂H₇₃ClO₂Pd: C, 63.23; H, 9.22. Found: C, 63.48; H, 9.47.

Synthesis of 12. In a nitrogen-filled glovebox, a tared 4 mL screw-cap vial was charged with Pd(PCy₃)₂ (100 mg, 0.150 mmol) and a stirbar. A second 4 mL vial was charged with **11** (25.0 mg, 0.158 mmol) and heptane (1 mL). The solution of **11** was transferred to the vial containing Pd(PCy₃)₂, using two additional portions of heptane (0.5 mL each), to effect a quantitative transfer. The mixture changed color to brown/orange immediately upon addition of the acid chloride. The suspension was stirred and became homogeneous after approximately 10 min. At this point, an orange solid began to precipitate; stirring was continued for a further 2 h, after which the vial was placed in a -35 °C freezer for several days. After standing, the mother liquor was decanted and the orange solid washed with pentane (2 × 1 mL) and dried in vacuo. The solid was again triturated with pentane to remove residual toluene solvent and dried extensively in vacuo to give compound **12** (79.3 mg, 64% yield). ¹H NMR (400 MHz, d₈-toluene): δ (ppm) 1.04–1.34 (m, 18 H, 18 × Cy-H), 1.53–1.83 (m, 32 H, $-\text{CH}_2\text{CH}_2\text{C}=\text{CH}-$, 30 × Cy-H), 1.90–2.04 (m, 6 H, 6 × PCHR₂), 2.13–2.36 (m, 14 H, $-\text{CH}_2\text{C}=\text{CH}-$, 12 × Cy-H), 2.45 (br t, *J* = 5.30 Hz, 2 H, $-\text{CH}_2\text{C}=\text{O}$), 7.99 (s, 1 H, $-\text{C}=\text{CH}-$). ¹³C{¹H} NMR (101 MHz, d₈-toluene): δ (ppm) 27.60, 30.05, 31.60, 32.60–33.05 (m, 3 C overlapping), 35.18 (d, *J* = 22.6 Hz), 39.60 (t, *J* = 8.90 Hz), 43.60, 146.74 (br), 165.17 (t, *J* = 11.60 Hz), 204.12, 240.53. ³¹P{¹H} NMR (162 MHz, d₈-toluene) δ (ppm) 21.44. LRMS (ESI): obtained using LCMS under standard conditions; fragment observed between *m/z* 787 and 795 in diagnostic isotope pattern, with most intense peak at *m/z* 789.8, corresponding to [Pd(PCy₃)₂(COR)]⁺; most intense fragment peak observed at *m/z* 281 for [HPCy₃]⁺. These isotope patterns are pictured in the Supporting Information. Anal. Calcd for C₄₃H₇₃ClO₂Pd: C, 62.54; H, 8.91. Found: C, 62.80; H, 9.19.

■ ASSOCIATED CONTENT

Supporting Information

The Supporting Information is available free of charge on the ACS Publications website at DOI: 10.1021/acs.organomet.8b00468.

Detailed experimental procedures, full tables of screening data, characterization data, reaction progress plots, and crystallographic details (PDF)

Accession Codes

CCDC 1852940–1852941 contain the supplementary crystallographic data for this paper. These data can be obtained free of charge via www.ccdc.cam.ac.uk/data_request/cif, or by emailing data_request@ccdc.cam.ac.uk, or by contacting The Cambridge Crystallographic Data Centre, 12 Union Road, Cambridge CB2 1EZ, UK; fax: +44 1223 336033.

■ AUTHOR INFORMATION

Corresponding Author

*E-mail for D.C.L.: david.c.leitch@gsk.com; dcleitch@uvic.ca.

ORCID

Anna L. Dunn: 0000-0003-2852-7755

Graham E. Dobereiner: 0000-0001-6885-2021

David C. Leitch: 0000-0002-8726-3318

Notes

The authors declare no competing financial interest.

■ ACKNOWLEDGMENTS

The authors thank Dr. Ian Andrews, Dr. Alexander O'Brien, Dr. Praew Thansandote, and Dr. Antonella Carangio for insightful discussions and Dr. Bernie O'Hare for assistance with NMR experiments. Analytical data were obtained from the CENTC Elemental Analysis Facility at the University of Rochester, funded by NSF CHE-0650456. This material is based upon work supported by the National Science Foundation under Grant No. CHE-1565721.

■ REFERENCES

- (1) (a) *Catalytic Carbonylation Reactions*; Beller, M., Ed.; Springer-Verlag: Berlin, 2006. (b) Beller, M.; Wu, X.-F. *Transition Metal Catalyzed Carbonylation Reactions*; Springer-Verlag: Berlin, 2013.
- (2) Appel, A. M.; Bercaw, J. E.; Bocarsly, A. B.; Dobbek, H.; DuBois, D. L.; Dupuis, M.; Ferry, J. G.; Fujita, E.; Hille, R.; Kenis, P. J. A.; Kerfeld, C. A.; Morris, R. H.; Peden, C. H. F.; Portis, A. R.; Ragsdale, S. W.; Rauchfuss, T. B.; Reek, J. N. H.; Seefeldt, L. C.; Thauer, R. K.; Waldropa, G. L. Frontiers, Opportunities, and Challenges in Biochemical and Chemical Catalysis of CO₂ Fixation. *Chem. Rev.* **2013**, *113*, 6621–6658.
- (3) (a) Franke, R.; Selent, D.; Börner, A. Applied Hydroformylation. *Chem. Rev.* **2012**, *112*, S675–S732. (b) de Vries, J. G. Hydroformylation of Alkenes: Industrial Applications. In *Science of Synthesis: C-1 Building Blocks in Organic Synthesis*; van Leeuwen, P. W. N. M., Ed.; Georg Thieme Verlag: Stuttgart, 2014; Vol. 1, pp 193–228.
- (4) (a) Howard, M. J.; Jones, M. D.; Roberts, M. S.; Taylor, S. A. C1 to acetyls: catalysis and process. *Catal. Today* **1993**, *18*, 325–354. (b) Sunley, G. J.; Watson, D. J. High productivity methanol carbonylation catalysis using iridium: The Cativa process for the manufacture of acetic acid. *Catal. Today* **2000**, *58*, 293–307. (c) Zoeller, J. R. 2015 Paul N. Rylander Award Address: Selected Advances in Catalysis and Reactor Systems for the Generation of Acetates and Propionates Using Carbonylation. *Org. Process Res. Dev.* **2016**, *20*, 1016–1025.
- (5) (a) Barnard, C. F. J. Palladium-Catalyzed Carbonylation—A Reaction Come of Age. *Organometallics* **2008**, *27*, S402–S422. (b) Grigg, R.; Mutton, S. P. Pd-catalysed carbonylations: versatile technology for discovery and process chemists. *Tetrahedron* **2010**, *66*, 5515–5548. (c) Magano, J.; Dunetz, J. R. Large-Scale Applications of Transition Metal-Catalyzed Couplings for the Synthesis of Pharmaceuticals. *Chem. Rev.* **2011**, *111*, 2177–2250. (d) Wu, L.; Fang, X.; Liu, Q.; Jackstell, R.; Beller, M.; Wu, X.-F. Palladium-Catalyzed Carbonylative Transformation of C(sp³)–X Bonds. *ACS Catal.* **2014**, *4*, 2977–2989. (e) Neumann, H.; Schranck, J. Carbonylation of Aryl and Vinyl Halides. In *Science of Synthesis: C-1 Building Blocks in Organic Synthesis*; van Leeuwen, P. W. N. M., Ed.; Georg Thieme Verlag: Stuttgart, 2014; Vol. 2, pp 67–93. (f) Bai, Y.; Davis, D. C.; Dai, M. Natural Product Synthesis via Palladium-Catalyzed Carbonylation. *J. Org. Chem.* **2017**, *82*, 2319–2328.
- (6) Labinger, J. Tutorial on Oxidative Addition. *Organometallics* **2015**, *34*, 4784–4795.
- (7) (a) Huser, M.; Youinou, M.-T.; Osborn, J. A. Chlorocarbon Activation: Catalytic Carbonylation of Dichloromethane and Chlorobenzene. *Angew. Chem., Int. Ed. Engl.* **1989**, *28*, 1386–1388. (b) Ben-David, Y.; Portnoy, M.; Milstein, D. Chelate-assisted, palladium-catalyzed efficient carbonylation of aryl chlorides. *J. Am. Chem. Soc.* **1989**, *111*, 8742–8744. (c) Ben-David, Y.; Portnoy, M.; Milstein, D. Formylation of aryl chlorides catalysed by a palladium complex. *J. Chem. Soc., Chem. Commun.* **1989**, 1816–1817.

- (d) Grushin, V. V.; Alper, H. An exceptionally simple biphasic method for the metal catalysed carbonylation of chloroarenes. *J. Chem. Soc., Chem. Commun.* **1992**, 611–612. (e) Portnoy, M.; Milstein, D. Chelate effect on the structure and reactivity of electron-rich palladium complexes and its relevance to catalysis. *Organometallics* **1993**, *12*, 1655–1664. (f) Mägerlein, W.; Indolese, A. F.; Beller, M. A More Efficient Catalyst for the Carbonylation of Chloroarenes. *Angew. Chem., Int. Ed.* **2001**, *40*, 2856–2859. (g) Beller, M.; Mägerlein, W.; Indolese, A. F.; Fischer, C. Efficient Palladium-Catalyzed Alkoxy-carbonylation of N-Heteroaryl Chlorides - A Practical Synthesis of Building Blocks for Pharmaceuticals and Herbicides. *Synthesis* **2001**, *2001*, 1098–1109. (h) Mägerlein, W.; Indolese, A. F.; Beller, M. Development of new palladium catalysts for the alkoxy-carbonylation of aryl chlorides. *J. Organomet. Chem.* **2002**, *641*, 30–40. (i) Jimenez-Rodriguez, C.; Eastham, G. R.; Cole-Hamilton, D. J. The methoxycarbonylation of aryl chlorides catalysed by palladium complexes of bis(di-tert-butylphosphinomethyl)-benzene. *Dalton Trans.* **2005**, 1826–1830. (j) Cai, C.; Rivera, N. R.; Balsells, J.; Sidler, R. R.; McWilliams, J. C.; Shultz, C. S.; Sun, Y. An Efficient Catalyst for Pd-Catalyzed Carbonylation of Aryl Arenesulfonates. *Org. Lett.* **2006**, *8*, 5161–5164. (k) Watson, D. A.; Fan, X.; Buchwald, S. L. Carbonylation of Aryl Chlorides with Oxygen Nucleophiles at Atmospheric Pressure. Preparation of Phenyl Esters as Acyl Transfer Agents and the Direct Preparation of Alkyl Esters and Carboxylic Acids. *J. Org. Chem.* **2008**, *73*, 7096–7101. (l) Munday, R. H.; Martinelli, J. R.; Buchwald, S. L. Palladium-Catalyzed Carbonylation of Aryl Tosylates and Mesylates. *J. Am. Chem. Soc.* **2008**, *130*, 2754–2755. (m) Burhardt, M. N.; Taaning, R.; Nielsen, N. C.; Skrydstrup, T. Isotope-Labeling of the Fibril Binding Compound FSB via a Pd-Catalyzed Double Alkoxy-carbonylation. *J. Org. Chem.* **2012**, *77*, 5357–5363. (n) Chung, S.; Sach, N.; Choi, C.; Yang, X.; Drozda, S. E.; Singer, R. A.; Wright, S. W. Amino-carbonylation of Aryl Tosylates to Carboxamides. *Org. Lett.* **2015**, *17*, 2848–2851. (o) Wu, X.-F. Palladium-catalyzed carbonylative transformation of aryl chlorides and aryl tosylates. *RSC Adv.* **2016**, *6*, 83831–83837. (p) Wang, J. Y.; Strom, A. E.; Hartwig, J. F. Mechanistic Studies of Palladium-Catalyzed Aminocarbonylation of Aryl Chlorides with Carbon Monoxide and Ammonia. *J. Am. Chem. Soc.* **2018**, *140*, 7979–7993.
- (8) (a) Bougioukou, D. J.; Kille, S.; Taglieber, A.; Reetz, M. T. Directed Evolution of an Enantioselective Enoate-Reductase: Testing the Utility of Iterative Saturation Mutagenesis. *Adv. Synth. Catal.* **2009**, *351*, 3287–3305. (b) Turrini, N. G.; Cioc, R. C.; van der Niet, D. J. H.; Ruijter, E.; Orru, R. V. A.; Hall, M.; Faber, K. Biocatalytic access to nonracemic γ -oxo esters via stereoselective reduction using ene-reductases. *Green Chem.* **2017**, *19*, 511–518. (c) Hadi, T.; Diaz-Rodriguez, A.; Khan, D.; Morrison, J. P.; Kaplan, J. M.; Gallagher, K. T.; Schober, M.; Webb, M. R.; Brown, K.; Fuerst, D.; Snajdrova, R.; Roiban, G.-D. Identification and Implementation of Biocatalytic Transformations in Route Discovery: Synthesis of Chiral 1,3-Substituted Cyclohexanone Building Blocks. *Org. Process Res. Dev.* **2018**, *22*, 871.
- (9) (a) Zhang, H.-J.; Hu, L.; Ma, Z.; Li, R.; Zhang, Z.; Tao, C.; Cheng, B.; Li, Y.; Wang, H.; Zhai, H. Total Synthesis of the Diterpenoid (+)-Harringtonolide. *Angew. Chem., Int. Ed.* **2016**, *55*, 11638–11641. (b) Liu, Y.; Cheng, L.-J.; Yue, H.-T.; Che, W.; Xie, J.-H.; Zhou, Q.-L. Divergent enantioselective synthesis of hapalindole-type alkaloids using catalytic asymmetric hydrogenation of a ketone to construct the chiral core structure. *Chem. Sci.* **2016**, *7*, 4725–4729. (c) Nicolaou, K. C.; Liu, G.; Beabout, K.; McCurry, M. D.; Shamoo, Y. Asymmetric Alkylation of Anthrones, Enantioselective Total Synthesis of (–)- and (+)-Viridicatumtoxins B and Analogues Thereof: Absolute Configuration and Potent Antibacterial Agents. *J. Am. Chem. Soc.* **2017**, *139*, 3736–3746.
- (10) (a) Agosta, W. C.; Lowrance, W. W., Jr. Synthesis and Photocycloadditions of Compounds Related to 3-Carboxycyclohexenone. *J. Org. Chem.* **1970**, *35*, 3851–3856. (b) Lange, G. L.; Decicco, C.; Tan, S. L.; Chamberlain, G. Asymmetric Induction in Simple [2 + 2] Photoadditions. *Tetrahedron Lett.* **1985**, *26*, 4707–4710.
- (c) Webster, F. X.; Silverstein, R. M. Synthesis of Optically Pure Enantiomers of Grandisol. *J. Org. Chem.* **1986**, *51*, 5226–5231. (d) Herzog, H.; Koch, H.; Scharf, H. D.; Runsink, J. Chiral induction in photochemical reactions. V. Regio- and diastereoselectivity in the photochemical [2 + 2] cycloaddition of chiral cyclenone-3-carboxylates with 1,1'-diethoxyethene. *Tetrahedron* **1986**, *42*, 3547–3558. (e) Herzog, H.; Koch, H.; Scharf, H. D.; Runsink, J. Chiral induction in photochemical reactions. VII. Double stereodifferentiation in the [2 + 2] photocycloaddition. *Chem. Ber.* **1987**, *120*, 1737–1740. (f) Audenaert, F.; De Keukeleire, D.; Vandewalle, M. A new and facile perhydroazulene formation: the total synthesis of the carotane (+)-daucene. *Tetrahedron* **1987**, *43*, 5593–5604. (g) Lange, G. L.; Decicco, C. Asymmetric induction in mixed photoadditions employing α,β -unsaturated homochiral ketals. *Tetrahedron Lett.* **1988**, *29*, 2613–2614. (h) Lange, G. L.; Decicco, C. P.; Willson, J.; Strickland, L. A. Ring expansions of [2 + 2] photoadducts. Potential applications in the synthesis of triquinane and taxane skeletons. *J. Org. Chem.* **1989**, *54*, 1805–1810. (i) Lange, G. L.; Organ, M. G.; Lee, M. Reversal of regioselectivity with increasing ring size of alkene component in [2 + 2] photoadditions. *Tetrahedron Lett.* **1990**, *31*, 4689–4692. (j) Lange, G. L.; Gottardo, C. Free radical fragmentation of derivatives of [2 + 2] photoadducts. *Tetrahedron Lett.* **1990**, *31*, 5985–5988. (k) Lange, G. L.; Gottardo, C. Free Radical Fragmentation of [2 + 2] Photoadduct Derivatives. Formal Synthesis of Pentalenene. *J. Org. Chem.* **1995**, *60*, 2183–2187. (l) Omar, H. I.; Odo, Y.; Shigemitsu, Y.; Shimo, T.; Somekawa, K. Transition state analysis on regioselectivity in [2 + 2] photocycloaddition reactions of substituted 2-cyclohexenone with cycloalkenecarboxylates. *Tetrahedron* **2003**, *59*, 8099–8105. (m) Zhao, G.; Yang, C.; Sun, H.; Lin, R.; Xia, W. (+)-Camphor Derivative Induced Asymmetric [2 + 2] Photoaddition Reaction. *Org. Lett.* **2012**, *14*, 776–779.
- (11) (a) Brown, M. K.; May, T. L.; Baxter, C. A.; Hoveyda, A. H. All-Carbon Quaternary Stereogenic Centers by Enantioselective Cu-Catalyzed Conjugate Additions Promoted by a Chiral N-Heterocyclic Carbene. *Angew. Chem., Int. Ed.* **2007**, *46*, 1097–1100. (b) Shintani, R.; Tsutsumi, Y.; Nagaosa, M.; Nishimura, T.; Hayashi, T. Sodium Tetraarylborates as Effective Nucleophiles in Rhodium/Diene-Catalyzed 1,4-Addition to β,β -Disubstituted α,β -Unsaturated Ketones: Catalytic Asymmetric Construction of Quaternary Carbon Stereocenters. *J. Am. Chem. Soc.* **2009**, *131*, 13588–13589.
- (12) Izawa, Y.; Zheng, C.; Stahl, S. Aerobic Oxidative Heck/Dehydrogenation Reactions of Cyclohexenones: Efficient Access to meta-Substituted Phenols. *Angew. Chem., Int. Ed.* **2013**, *52*, 3672–3675.
- (13) (a) Lange, G. L.; Otulakowski, J. A. Improved preparation of methyl 3-oxo-1-cyclohexene-1-carboxylate and its use in the synthesis of substituted 1,5-cyclodecadienes. *J. Org. Chem.* **1982**, *47*, 5093–5096. (b) For a Rh-catalyzed allylic oxidation, see: Catino, A. J.; Forslund, R. E.; Doyle, M. P. Dirhodium(II) Caprolactamate: An Exceptional Catalyst for Allylic Oxidation. *J. Am. Chem. Soc.* **2004**, *126*, 13622–13623.
- (14) Webster, F. X.; Silverstein, R. M. Control of the Birch Reduction of m-Anisic Acid to Produce Specific 3-Oxocyclohexenecarboxylic Acids. *Synthesis* **1987**, *1987*, 922–924.
- (15) The only previously reported examples of β -halo enone carbonylation utilize either iodo or bromo leaving groups: (a) Baillargeon, V. P.; Stille, J. K. Direct conversion of organic halides to aldehydes with carbon monoxide and tin hydride catalyzed by palladium. *J. Am. Chem. Soc.* **1983**, *105*, 7175–7176. (b) Baillargeon, V. P.; Stille, J. K. Palladium-catalyzed formylation of organic halides with carbon monoxide and tin hydride. *J. Am. Chem. Soc.* **1986**, *108*, 452–461. (c) Kuethe, J. T.; Wong, A.; Wu, J.; Davies, I. W.; Dormer, P. G.; Welch, C. J.; Hillier, M. C.; Hughes, D. L.; Reider, P. J. Asymmetric Synthesis of 1,2,3-Trisubstituted Cyclopentanes and Cyclohexanes as Key Components of Substance P Antagonists. *J. Org. Chem.* **2002**, *67*, 5993–6000. (d) Ebner, D. C.; Bagdanoff, J. T.; Ferreira, E. M.; McFadden, R. M.; Caspi, D. D.; Trend, R. M.; Stoltz, B. M. The Palladium-Catalyzed Aerobic Kinetic

Resolution of Secondary Alcohols: Reaction Development, Scope, and Applications. *Chem. - Eur. J.* **2009**, *15*, 12978–12992.

(16) Buitrago Santanilla, A.; Regalado, E. L.; Pereira, T.; Shevlin, M.; Bateman, K.; Campeau, L.-C.; Schneeweis, J.; Berrit, S.; Shi, Z.-C.; Nantermet, P.; Liu, Y.; Helmy, R.; Welch, C. J.; Vachal, P.; Davies, I. W.; Cernak, T.; Dreher, S. D. Nanomole-scale high-throughput chemistry for the synthesis of complex molecules. *Science* **2015**, *347*, 49–53.

(17) (a) Klaus, S.; Neumann, H.; Zapf, A.; Strübing, D.; Hübner, S.; Almena, J.; Riermeier, T.; Gross, P.; Sarich, M.; Krahnert, W.-R.; Rossen, K.; Beller, M. A General and Efficient Method for the Formylation of Aryl and Heteroaryl Bromides. *Angew. Chem., Int. Ed.* **2006**, *45*, 154–158. (b) Barnard, C. F. J. Carbonylation of Aryl Halides: Extending the Scope of the Reaction. *Org. Process Res. Dev.* **2008**, *12*, 566–574. (c) Martinelli, J. R.; Watson, D. A.; Freckmann, D. M. M.; Barder, T. E.; Buchwald, S. L. Palladium-Catalyzed Carbonylation Reactions of Aryl Bromides at Atmospheric Pressure: A General System Based on Xantphos. *J. Org. Chem.* **2008**, *73*, 7102–7107. (d) Arthuis, M.; Lecup, A.; Roulland, E. Pd₀-Catalyzed carbonylation of 1,1-dichloro-1-alkenes, a new selective access to Z- α -chloroacrylates. *Chem. Commun.* **2010**, *46*, 7810–7812. (e) Quesnel, J. S.; Arndtsen, B. A. A Palladium-Catalyzed Carbonylation Approach to Acid Chloride Synthesis. *J. Am. Chem. Soc.* **2013**, *135*, 16841–16844.

(18) Netherton, N. R.; Fu, G. C. Air-Stable Trialkylphosphonium Salts: Simple, Practical, and Versatile Replacements for Air-Sensitive Trialkylphosphines. Applications in Stoichiometric and Catalytic Processes. *Org. Lett.* **2001**, *3*, 4295–4298.

(19) See the [Supporting Information](#) for more details.

(20) For examples of chemoselective Pd-catalyzed functionalizations of R–Cl over R–Br groups in noncarbonylative cross couplings, see: (a) Almond-Thynne, J.; Blakemore, D. C.; Pryde, D. C.; Spivey, A. C. Site-selective Suzuki–Miyaura coupling of heteroaryl halides – understanding the trends for pharmaceutically important classes. *Chem. Sci.* **2017**, *8*, 40–62. (b) Keylor, M. H.; Niemeyer, Z. L.; Sigman, M. S.; Tan, K. L. Inverting Conventional Chemoselectivity in Pd-Catalyzed Amine Arylations with Multiply Halogenated Pyridines. *J. Am. Chem. Soc.* **2017**, *139*, 10613–10616.

(21) Nunn, C.; DiPietro, A.; Hodnett, N.; Sun, P.; Wells, K. M. High-Throughput Automated Design of Experiment (DoE) and Kinetic Modeling to Aid in Process Development of an API. *Org. Process Res. Dev.* **2018**, *22*, 54–61.

(22) (a) Littke, A. F.; Dai, C.; Fu, G. C. Versatile Catalysts for the Suzuki Cross-Coupling of Arylboronic Acids with Aryl and Vinyl Halides and Triflates under Mild Conditions. *J. Am. Chem. Soc.* **2000**, *122*, 4020–4028. (b) Christmann, U.; Vilar, R. Monoligated palladium species as catalysts in cross-coupling reactions. *Angew. Chem., Int. Ed.* **2005**, *44*, 366–374.

(23) Meng, G.; Szostak, M. General Olefin Synthesis by the Palladium-Catalyzed Heck Reaction of Amides: Sterically Controlled Chemoselective N–C Activation. *Angew. Chem., Int. Ed.* **2015**, *54*, 14518–14522 and references therein.

(24) (a) Galardon, E.; Ramdeehul, S.; Brown, J. M.; Cowley, A.; Hii, K. K. M.; Jutand, A. Profound Steric Control of Reactivity in Aryl Halide Addition to Bisphosphane Palladium(0) Complexes. *Angew. Chem., Int. Ed.* **2002**, *41*, 1760–1763. (b) Barrios-Landeros, F.; Hartwig, J. F. Distinct Mechanisms for the Oxidative Addition of Chloro-, Bromo-, and Iodoarenes to a Bisphosphine Palladium(0) Complex with Hindered Ligands. *J. Am. Chem. Soc.* **2005**, *127*, 6944–6945. (c) Barrios-Landeros, F.; Carrow, B. P.; Hartwig, J. F. Effect of Ligand Steric Properties and Halide Identity on the Mechanism for Oxidative Addition of Haloarenes to Trialkylphosphine Pd(0) Complexes. *J. Am. Chem. Soc.* **2009**, *131*, 8141–8154. (d) Mitchell, E. A.; Jessop, P. G.; Baird, M. C. A Kinetics Study of the Oxidative Addition of Bromobenzene to Pd(PCy₃)₂ (Cy = cyclohexyl) in a Nonpolar Medium: The Influence on Rates of Added PCy₃ and Bromide Ion. *Organometallics* **2009**, *28*, 6732–6738. (e) Kurbangalieva, A.; Carmichael, D.; Hii, K. K. M.; Jutand, A.; Brown, J. M. Oxidative Addition to Palladium(0) Diphosphine Complexes:

Observations of Mechanistic Complexity with Iodobenzene as Reactant. *Chem. - Eur. J.* **2014**, *20*, 1116–1125.

(25) (a) Kirchoff, J. H.; Netherton, M. R.; Hills, I. D.; Fu, G. C. Boronic Acids: New Coupling Partners in Room-Temperature Suzuki Reactions of Alkyl Bromides. Crystallographic Characterization of an Oxidative-Addition Adduct Generated under Remarkably Mild Conditions. *J. Am. Chem. Soc.* **2002**, *124*, 13662–13663. (b) Mitchell, E. A.; Baird, M. C. Optimization of Procedures for the Syntheses of Bisphosphinepalladium(0) Precursors for Suzuki–Miyaura and Similar Cross-Coupling Catalysis: Identification of 3:1 Coordination Compounds in Catalyst Mixtures Containing Pd(0), PCy₃, and/or P^tMeBu₂. *Organometallics* **2007**, *26*, 5230–5238.

(26) Majchrzak, M.; Kostera, S.; Kubicki, M.; Kownacki, I. Synthesis of new styrylarenes via Suzuki–Miyaura coupling catalysed by highly active, well-defined palladium catalysts. *Dalton Trans.* **2013**, *42*, 15535–15539.

(27) Wang, Z.; Orellana, A. Convenient Access to meta-Substituted Phenols by Palladium-Catalyzed Suzuki–Miyaura Cross-Coupling and Oxidation. *Chem. - Eur. J.* **2017**, *23*, 11445–11449.